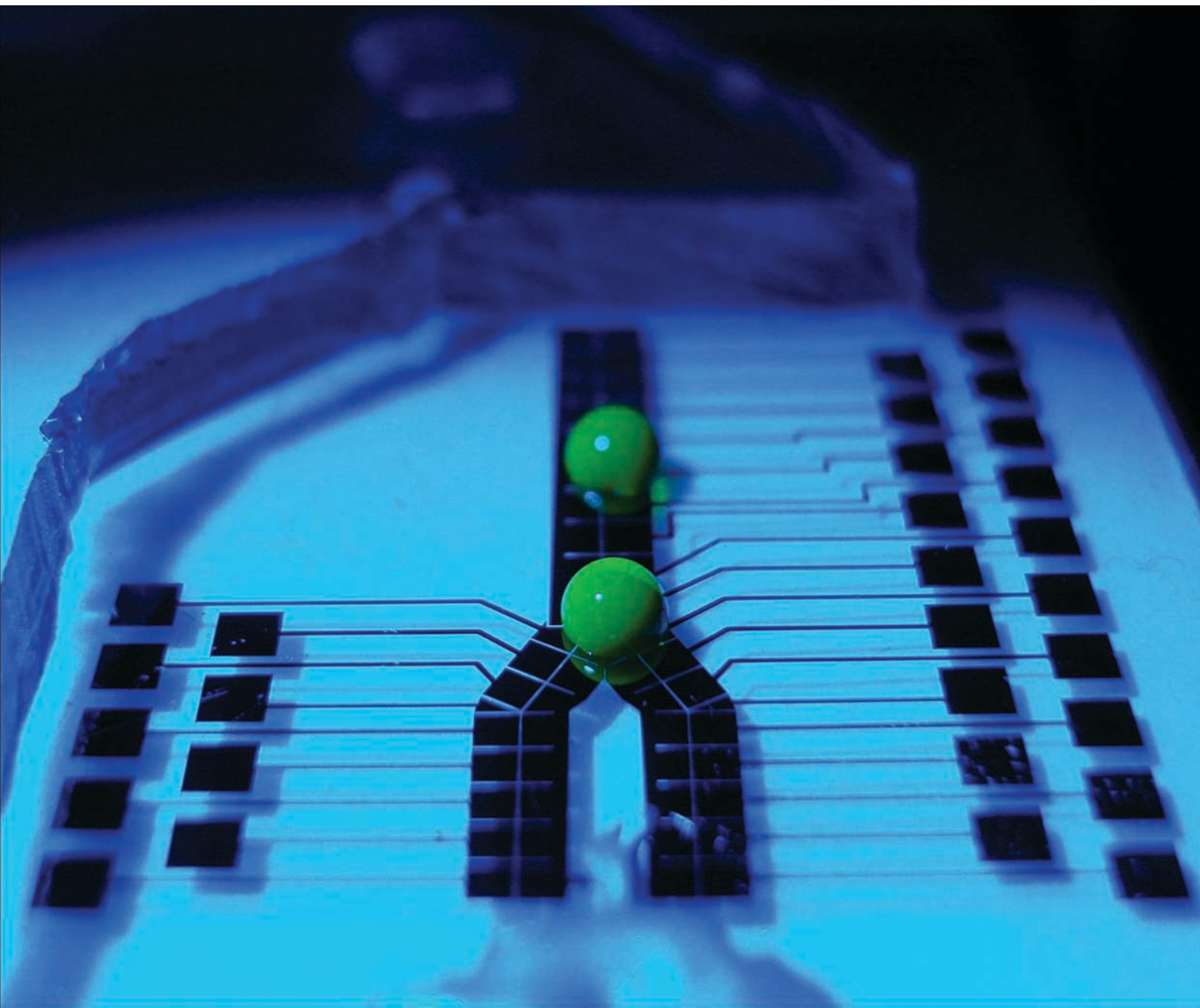


Lab on a Chip

Miniaturisation for chemistry, physics, biology, & bioengineering

www.rsc.org/loc

Volume 9 | Number 8 | 21 April 2009 | Pages 1021–1152



ISSN 1473-0197

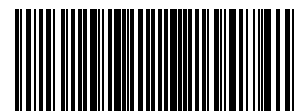
Wheeler
Microchannel–digital interface

Soh
Microdevice for phage selection

Okada
Lab on ice

Matsunaga
SNP genotyping from whole blood

RSC Publishing



1473-0197(2009)9:8;1-U

Hybrid microfluidics: A digital-to-channel interface for in-line sample processing and chemical separations

Mohamed Abdelgawad,^{†a} Michael W. L. Watson^{†b} and Aaron R. Wheeler^{*bcd}

Received 19th November 2008, Accepted 27th January 2009

First published as an Advance Article on the web 18th February 2009

DOI: 10.1039/b820682a

Microchannels can separate analytes faster with higher resolution, higher efficiency and with lower reagent consumption than typical column techniques. Unfortunately, an impediment in the path toward fully integrated microchannel-based labs-on-a-chip is the integration of pre-separation sample processing. Although possible in microchannels, such steps are challenging because of the difficulty in maintaining spatial control over many reagents simultaneously. In contrast, the alternative format of digital microfluidics (DMF), in which discrete droplets are manipulated on an array of electrodes, is well-suited for carrying out sequential chemical reactions. Here, we report the development of the first digital-channel hybrid microfluidic device for integrated pre-processing reactions and chemical separations. The device was demonstrated to be useful for on-chip labeling of amino acids and primary amines in cell lysate, as well as enzymatic digestion of peptide standards, followed by separation in microchannels. Given the myriad applications requiring pre-processing and chemical separations, the hybrid digital-channel format has the potential to become a powerful new tool for micro total analysis systems.

Introduction

Microchannels have revolutionized analytical separations, facilitating fast analyses with higher resolution, higher efficiency, and lower reagent consumption relative to their macro-scale counterparts.¹ In this capacity, microchannel-based methods have been used to separate mixtures of analytes ranging from small molecules like amino acids and neurotransmitters to large molecules like DNA and proteins.² To complement chemical separations, microchannel-based systems have been developed incorporating pre-column reactions, including enzymatic digestion,³ organic synthesis,⁴ and fluorescent derivatization.^{5,6} These techniques represent the promise of microfluidics for forming fully integrated labs-on-a-chip.

Unfortunately, the number and scope of labs-on-a-chip capable of integrating pre-column reactions with separations is limited. For example, there are no microfluidic methods reported that could be useful for shotgun proteomics, in which samples are subjected to a rigorous, multi-step processing regimen requiring several days to complete.⁷ This deficit is largely mechanistic—managing multiple reagents with precise control over position and reaction time in microchannels is complicated by the near-universal effects of hydrostatic and capillary flows.^{8–10} The development of integrated microvalves¹¹ offers some relief from

this problem; however, the complicated fabrication and control infrastructure required for this technology has limited its widespread use.¹² Another technique that might be useful for pre-column reactions and separations is multi-phase microfluidic systems (*i.e.*, droplets in channels).¹³ In recent work, Edgar *et al.*¹⁴ and Roman *et al.*¹⁵ reported methods capable of delivering droplets from such systems directly into separation channels. This is an exciting new development, but we posit that the droplets-in-channels paradigm is not ideally suited for controlling multistep chemical reactions, as droplets (regardless of their contents) are typically controlled in series.

Here, we introduce a new method for integrated chemical processing and separations, relying on digital microfluidics (DMF). Digital microfluidics is a distinct paradigm from droplets-in-channels—in DMF, droplets are manipulated on an open array of electrodes.^{16,17} DMF is well-suited for carrying out sequential chemical reactions^{18–20} in which droplets containing different reagents^{21,22} and phases²³ can be dispensed from reservoirs, moved, split, and merged.²⁴ Most importantly, DMF facilitates precise temporal and spatial control over many different reagents simultaneously and independently.^{25,26} In the method presented here, we have integrated, for the first time, digital microfluidics on the front end of a microchannel-based system for separations.

The work reported here joins a small group of studies that have used digital microfluidics (or related techniques) in devices containing microchannels. In most of these studies, electro-wetting was used within channels to facilitate droplet generation²⁷ or to direct fluid flow.^{28–30} In another study (described in a conference proceedings paper³¹), a hybrid channel-to-digital microfluidic interface was reported (the “opposite” of what is described here). In that work, samples of fluid exiting a microchannel were collected into droplets that were then manipulated by DMF. While this is an exciting innovation, we believe that the

^aDepartment of Mechanical and Industrial Engineering, University of Toronto, 5 King's College Road, Toronto, Ontario M5S 3G8, Canada

^bDepartment of Chemistry, University of Toronto, 80 St. George Street, Toronto, Ontario M5S 3H6, Canada. E-mail: awheeler@chem.utoronto.ca; Fax: +416-946-3865; Tel: +416-946-3864

^cInstitute of Biomaterials and Biomedical Engineering, University of Toronto, 164 College Street, Toronto, Ontario M5S 3G9, Canada

^dBanting and Best Department of Medical Research, University of Toronto, 112 College Street, Toronto, Ontario M5G 1L6, Canada

[†] These authors contributed equally to this work.

unique capacity of DMF to precisely manage many different reagents makes it particularly attractive for pre-separation sample processing. Moreover, the disparity in volumes for the two techniques (typically 0.1–10 μL for DMF *vs.* \sim 0.01–1 nL for microchannels) suggests that DMF is a better match for pre-separation (as opposed to post-separation³¹) applications. In the following, we describe the first implementation of a digital-to-channel interface, and its application to sample processing and separations. We believe this may be an important step towards fully automated lab-on-a-chip methods suitable for a wide range of applications.

Experimental

Reagents and materials

Unless otherwise indicated all general-use chemicals were obtained from Sigma-Aldrich (Oakville, ON), and cell-culture reagents were from American Type Culture Collection (ATCC, Manassas, VA). Materials required for device fabrication included chromium pellets (Kurt J. Lesker Canada, Toronto, ON), hexamethyldisilazane (HMDS) (Shin-Etsu MicroSi (Phoenix, AZ), Shipley S1811 photoresist and MF321 developer (Rohm and Haas, Marlborough, MA), CR-4 chromium etchant (Cyantek, Fremont, CA), AZ300T stripper (AZ Electronic Materials, Summerville, NJ), parylene-C (Specialty Coating Systems, Indianapolis, IN), Teflon-AF1600 (DuPont, Wilmington, DE) and Fluorinert FC-40 (Sigma Aldrich, Oakville, ON). Materials for microchannel fabrication included SU-8-25 photoresist (MicroChem, Newton, CA), silicon wafers (Waferworld, West Palm Beach, FL), and polydimethylsiloxane (PDMS) (Sylgard-184 kits, Dow Corning, Midland, MI). Reagents used in cell culture experiments included fetal bovine serum and Trypan blue dye from Invitrogen Canada, (Burlington, ON). Other reagents included methanol and acetonitrile (ACP, Montreal, QC), fluorescein isothiocyanate monolabeled insulin (FITC-Ins) from Invitrogen-Molecular Probes (Eugene, OR), and food coloring dyes from McCormick Canada (London, ON).

Cell culture

HeLa cells were grown in a humidified incubator (5% CO_2 37 $^\circ\text{C}$) in Dulbecco's Modified Eagle Medium (DMEM) supplemented with fetal bovine serum (10%), penicillin (100 IU mL^{-1}), and streptomycin (100 $\mu\text{g mL}^{-1}$). Cells were subcultured every 3–4 days at $\sim 5 \times 10^3$ cells cm^{-2} seeding density. For lysis, cells were washed in phosphate buffered saline (PBS), then suspended (2×10^6 cells mL^{-1}) in lysing medium containing PBS with Pluronic F-68 (0.02% wt/v), Triton X-100 (1%), and PMSF (1 mM). After incubation on ice (30 min), the lysate was centrifuged (1250 $\times g$, 5 min) and the supernatant was collected and stored in a freezer (-85°C) until use.

Device fabrication

The method used to fabricate hybrid digital-channel microfluidic devices is depicted in Fig. 1. Digital microfluidic elements were formed from chromium (150 nm) on glass substrates in the University of Toronto Emerging Communications Technology

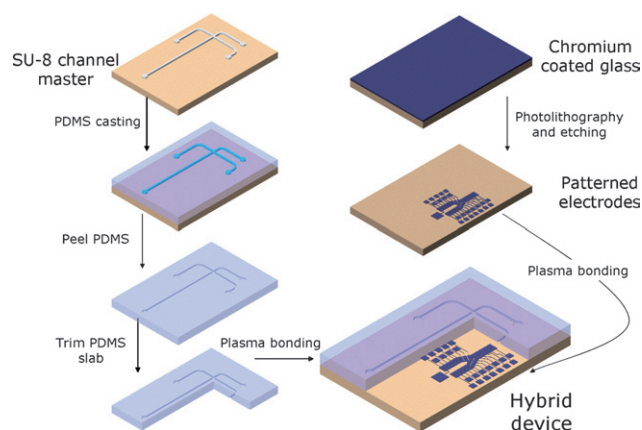


Fig. 1 Schematic of the fabrication protocol used to produce hybrid microfluidic devices. The parylene and Teflon coating steps are not shown.

Institute (ECTI). An array of electrodes was patterned by photolithography and wet etching in a “Y-shape” with electrode dimensions of 1 mm \times 1 mm in the branches and 1.2 mm \times 1.2 mm in the stem, with inter-electrode gaps of 25 μm . The microchannel network was formed by soft lithography, casting polydimethylsiloxane (PDMS) against an SU-8-on-silicon master in a method similar to that reported by Duffy *et al.*³² The channels were 40 μm deep \times 100 μm wide, and the layout included a cross element for injection and a 4.5 cm-long separation channel. After curing, holes were punched at the channel inlets to create fluid reservoirs in the \sim 3–4 mm-thick PDMS slab. The sample channel was exposed by slicing through the slab with a scalpel. The microchannel network was then bonded to the glass substrate carrying the electrode array after exposure to an oxygen plasma³² (90 s) such that the sample channel inlet mated with the edge of the electrode array—this formed the “digital-channel interface” (see Fig. 2). A layer of parylene-C (2 μm) was then deposited onto the electrode array. During deposition, the PDMS slab carrying the microchannel network was protected by covering with low-tack dicing tape (Semiconductor Equipment Corporation, Moorpark, CA), with special attention given to sealing the channel inlets. Although it was not necessary, protecting the top of the PDMS slab was useful for experiments, as the parylene coating blurs visualization through the microscope. Finally, a hydrophobic layer of Teflon AF (50 nm) was applied by spin coating (1% concentration in Fluorinert FC-40, 2000 rpm, 1 min) followed by baking on a hot plate (160 $^\circ\text{C}$, 10 min). In some cases, the edge of the dicing tape prevented the Teflon from coating the row of electrodes directly adjacent to the digital-channel interface. The dicing tape was removed when the device was ready for use.

Device operation

Prior to experiments, the network of microchannels was loaded with run buffer by filling one reservoir (50 μL) and gently applying positive pressure. After filling the channels, buffer was added to the reservoirs to balance the fluid heights to limit hydrostatic flow.⁸ Gentle pressure was applied to the run buffer reservoir, creating a small outward meniscus of fluid at the

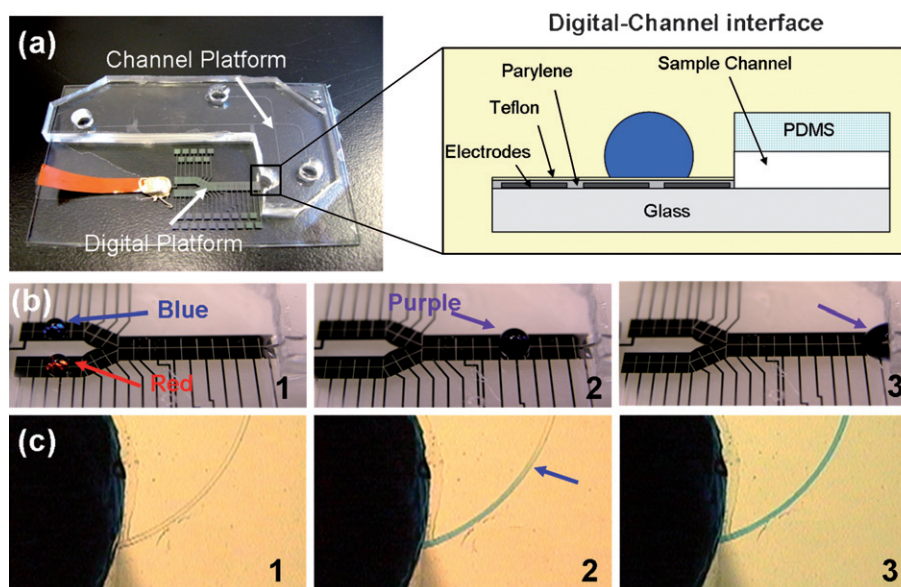


Fig. 2 Picture, schematic, and frames from movies depicting a hybrid digital-channel microfluidic device. (a) The hybrid device comprises an electrode array for sample preparation by digital microfluidics and a network of microchannels for chemical separations. The inset is a schematic of the interface (not to scale). (b) Frames from a movie (left-to-right) depicting droplets containing colored dyes being moved, merged, and mixed by DMF and then delivered to the interface. (c) Frames from a movie (left-to-right) demonstrating electrokinetic loading of the contents of a droplet into a microchannel. The arrow in panel 2 indicates the front of the reagent (purple dye) being loaded into the channel from the droplet.

digital-channel interface. Devices were used as described above, or, in some cases, supplemented with an additional buffer volume (45 μL) pipetted adjacent to the digital-channel interface to further balance the flow. Platinum wire electrodes (250 μm diameter) were inserted into each buffer reservoir as well as into the interface; the latter was pushed through the PDMS slab (such that the tip penetrated into the open space adjacent to the interface) to hold it in place. After preparing the microchannel platform, droplets (2.5 μL) were dispensed by pipette onto the electrodes and actuated by DMF in single-plate format.^{33,34} Driving potentials (100–300 V_{RMS} , 18 kHz) were generated by amplifying the output of a function generator and were applied to sequential pairs of electrodes to move, merge, and mix droplets. Droplet actuation was monitored and recorded by a Hitachi CCD camera mated to an imaging lens (Edmund Industrial Optics, Barrington, NJ).

After delivering a droplet to the interface by DMF, the contents were driven into the sample channel electrokinetically for pinched injections and separations. Electric fields were applied *via* a high voltage sequencer (LabSmith, Livermore, CA), and separations were performed in micellar electrokinetic chromatography (MEKC) mode in run buffer 1 (20 mM Borate pH 9.0, 50 mM SDS and 10% ACN) or run buffer 2 (20 mM borate pH 9.0, 25 mM SDS, 30% ACN). Analytes were detected by laser induced fluorescence using an inverted microscope (Olympus IX-71) mated to an argon ion laser (Melles Griot, Carlsbad, CA). The 488 nm laser line was used for green fluorescence (fluorescein, rhodamine and FITC-Ins), and the 457 nm line was used for blue fluorescence (NDA-derivatives). The laser was focused into the channel using an objective (60 \times); the fluorescent signal was collected by the same lens and filtered optically (536/40 nm band pass and 488 nm notch filter for green fluorescence and a 482/35 nm band pass and 457 nm notch filter for blue fluorescence) and

spatially (500 μm pinhole), and imaged onto a photomultiplier tube (Hamamatsu, Bridgewater, NJ). PMT current was converted to voltage using a picoammeter (Keithley Instruments, Cleveland, OH) and then collected using a DAQpad A–D converter (National Instruments, Austin, TX) and a PC running a custom LabVIEW (Natl. Inst.) program.

Analysis of reproducibility

The fluorescent dyes, rhodamine 123 and fluorescein, were used to evaluate separation performance and reproducibility. Samples containing both dyes (10 μM each, final concentration) were prepared (a) on-chip by merging one droplet containing rhodamine 123 and a second containing fluorescein, (b) off-chip in five independently prepared samples, and (c) off-chip from a single mixture. In each case, five replicates were loaded electrokinetically into microchannels and then separated by MEKC in run buffer 1. The resulting electropherograms were analyzed for peak area, retention time (t_R) and peak width at half-max ($W_{1/2}$) using PeakFit (SeaSolve Software Inc., Framingham, MA). For each run, the rhodamine 123 peak area was calculated relative to that of fluorescein and is listed as a percent relative standard deviation (% RSD). The number of theoretical plates, N , was calculated using $W_{1/2}$.

$$N = 5.54 \left(\frac{t_R}{W_{1/2}} \right)^2$$

NDA labeling

Amino acid standards and cell lysate were labeled on-chip with the fluorogenic dye, naphthalene-2,3-dicarboxyaldehyde (NDA) using potassium cyanide (KCN) as nucleophile. In these

experiments, two solutions were used, containing the analytes and the label, respectively. For on-chip labeling of amino acids, the former solution comprised glycine, alanine and valine standards (20 μM each with 4 mM KCN in run buffer 2), while the latter comprised NDA (2 mM in run buffer 2). For on-chip labeling of cell constituents, the analyte solution was formed by diluting a thawed aliquot of lysate 1 : 10 in run buffer 1 containing KCN (20 mM final concentration), while the reagent solution was NDA (10 mM) in neat acetonitrile. In each case, droplets of analyte and reagent solution were moved, merged, incubated (2 min), and then delivered to the digital-channel interface by DMF. Samples were then loaded and injected electrokinetically, followed by a separation using MEKC in run buffer 1 (lysate) or 2 (standards).

Lysate peaks were tentatively identified by standard additions of NDA-labeled amino acids. Briefly, amino acid standards (50 μM) were reacted off-line with KCN (2 mM) and NDA (1 mM) in borate buffer (50 mM, pH 9, 30% ACN). Lysate was labeled off-line using the same concentrations described above and diluted 1 : 10 in run buffer 1 prior to analysis. Aliquots of lysate (48 μL) were combined with aliquots of amino acid standards (2 μL) and separated by MEKC in run buffer 1 to identify co-eluting lysate analytes.

Tryptic digestion

Two solutions were used for evaluation of on-chip digestion: FITC-Ins (50 $\mu\text{g}/\text{mL}$) in borate buffer (50 mM, pH 9), and trypsin (100 $\mu\text{g}/\text{mL}$) in Tris-HCl buffer (10 mM, 1 mM CaCl_2 , 0.08% pluronic F-127, pH 8.5). Droplets of each solution were moved, merged, and mixed by DMF, and allowed to react for a designated period of time (1, 5, 15, and 30 min). During incubation, to limit the effects of evaporation, the reacting droplet was enclosed in a PDMS cover. After reaction, the processed insulin was delivered to the digital-channel interface by DMF, and loaded, injected, and separated by MEKC in run buffer 1.

Results and discussion

Device fabrication and operation

The principle of device operation is shown in Fig. 2. Droplets containing reagents were moved, merged, incubated (if needed), and then delivered to the channel network for separations. Droplet movement was facile and fast, facilitating rapid mixing of a wide range of samples, reagents, and buffers. Pluronic solution additives were used to limit non-specific adsorption and pinning to the surface,¹⁹ and for long incubation times (>1 min), evaporation was minimized by enclosing the droplet under a PDMS cover. In designing and building the devices reported here, we chose to use the single-plate DMF format, which is convenient for droplet delivery to the interface with microchannels. A drawback of the single-plate format is incompatibility with droplet dispensing from reservoirs; in future designs, that capacity might be added by including a two-plate to single-plate DMF interface, which has been reported previously.³⁵

After delivering a droplet to the channel inlet, the droplet's contents were loaded into the microchannel for separations. In most cases, reagents were loaded into pre-filled channels by

electrokinetic flow (as described in the methods section, an electrode was positioned such that it penetrated into the droplet at the interface); however, we also demonstrated that: (a) a droplet containing run buffer delivered to empty channels will fill the network by capillary action; and (b) a droplet delivered to pre-filled channels will spontaneously load by LaPlace pressure (similar to what has been reported previously¹⁰). We used electrokinetic loading because this was the most reliable method to inject samples onto the separation column. We note that in this method, only a small fraction of the fluid manipulated by DMF ($\sim 5 \mu\text{L}$ merged droplets) is sampled into the channels, and an even smaller fraction (<1 nL) is injected onto the separation column. In this capacity, the droplet serves an analogous role to on-chip reservoirs in conventional microchannel devices. In some applications, however, it may be desirable to capture a large fraction of the processed droplet for analysis—in such cases, a pre-concentrator might be integrated into the sample channel.^{36–38} Regardless, the results presented here represent an important step forward for such techniques—*i.e.*, the first digital-to-channel interface.

In initial experiments, we evaluated the new device for a simple mixing experiment—separate droplets containing rhodamine 123 or fluorescein were moved and merged, and the combined droplet was sampled into the channels for separation by MEKC. Typical separations data are shown in Fig. 3(a)—clearly, the original droplets were mixed, and both analytes were detected in

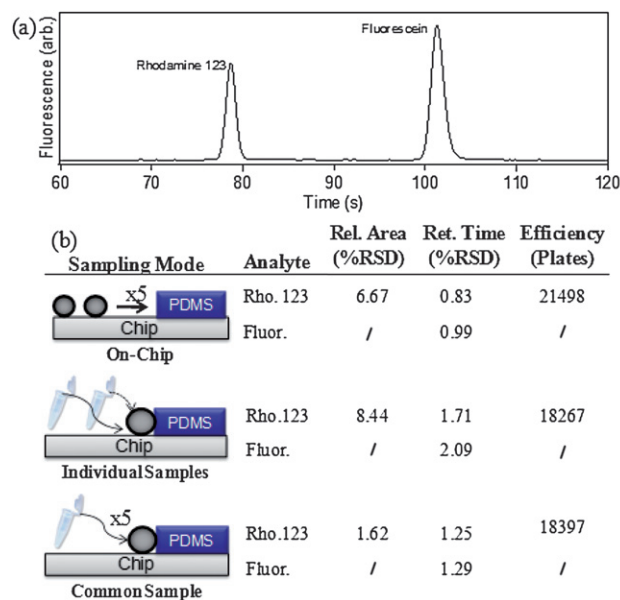


Fig. 3 Analysis of hybrid digital-channel microfluidic device reproducibility. In replicate experiments, droplets containing rhodamine 123 and fluorescein were combined on-chip and then evaluated by MEKC. A representative electropherogram is shown in (a), and reproducibility data are listed in (b). For comparison, two off-chip controls comprising replicate analyses of different mixtures (“individual samples”) and of a single mixture (“common sample”) were carried out, and the data are listed in (b). The observation that, in comparison with data generated from samples prepared on-chip, that the individual samples control has similar peak area reproducibility suggests that the main source of this variance is sample dispensing (*i.e.*, pipetting), rather than from chip operation.

the electropherogram. When evaluated in replicate trials, the method was characterized by excellent retention time reproducibility (<1% RSD) and separation efficiency (>20 000 plates over the 4.5 cm channel), but the relative peak area variation was larger than expected (~7% RSD). To probe the source of this error, we evaluated two controls, prepared off-chip. The first control (called “individual samples”), implemented to determine the variance caused by sample dispensing (*i.e.*, pipetting the two dye solutions), involved replicate measurements made from five individually prepared samples. Each sample contained run buffer (45 μ L), and rhodamine 123 and fluorescein (2.5 μ L each). The second control (called “common sample”), implemented to determine the variance caused by mixing, injection, and separation, involved replicate measurements from a single mixture of the two dyes. Cartoons depicting the controls and their respective data are listed in Fig. 3(b).

In comparing the performance of the on-chip method to the two controls, it appears that the primary source of peak area variance is sample dispensing (*i.e.*, pipetting). As listed in Fig. 3(b), the peak area reproducibility in the “individual samples” control is similar to that observed for the on-chip method, suggesting that the on-chip method and this control share the primary source of variance. In contrast, the peak area reproducibility in the “common sample” control is significantly improved, suggesting that the contribution to variance from mixing, injection, and separation, is much lower. Thus, we speculate that in future experiments with on-chip dispensing from reservoirs (instead of pipetting to the surface), the peak area reproducibility of the on-chip method will be substantially improved.

On-chip sample processing

To demonstrate the utility of the new device format for integrated sample processing, we used it to fluorescently label amino acid standards and cell lysate on-chip, followed by separations. For the former, a droplet containing the fluorogenic reagent, NDA, was merged with a droplet containing a mixture of three amino acid standards, glycine (Gly), alanine (Ala) and valine (Val), on the digital platform. The merged droplet was actuated between adjacent electrodes to mix its contents for ~2 min (comparable to reaction times reported for NDA labeling in microchannels³) and was then delivered to the interface where its contents were sampled into the channel by EOF. Fig. 4(a) shows an electropherogram generated using this method. Under these conditions, the three species separate in less than one minute.

A similar on-chip protocol was used to label the amines in a solution of cell lysate. As shown in Fig. 4(b), the constituent peaks are partially resolved in less than two minutes, and several of the peaks were tentatively assigned by spiking lysate mixtures with NDA-labeled amino acid standards. As expected, the more hydrophobic amino acids (*e.g.*, leucine) migrated slowly because of interaction with the micelles. Basic species such as arginine were likewise slowed as a function of electrophoretic migration in the opposite direction of the cathodic EOF.

To demonstrate a second sample processing application for the new device, we used it to digest a proteomic analyte prior to separation. Singly tagged FITC-Insulin (FITC-Ins) was a useful model for this work, as the single label simplifies the number of

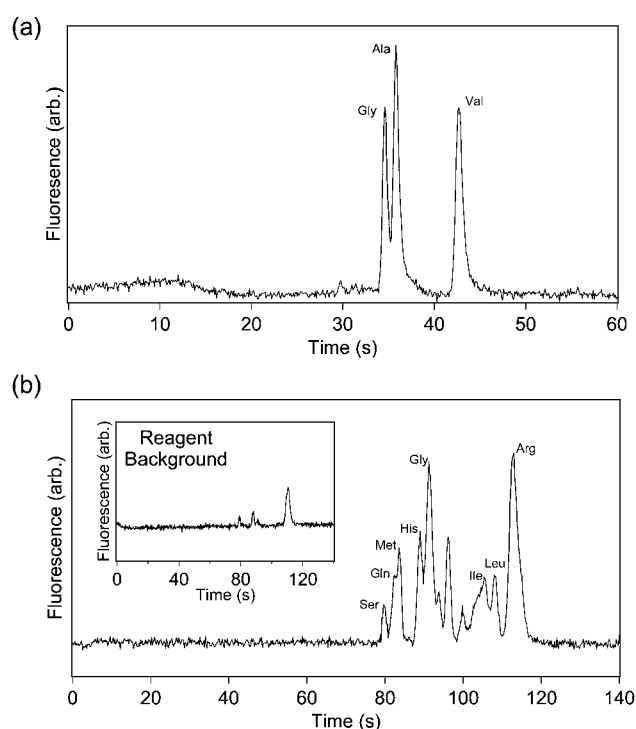


Fig. 4 Electropherograms generated after on-chip NDA labeling of amino acids and cell lysate. (a) Glycine (Gly), alanine (Ala) and valine (Val) (10 μ M ea.) were labeled with NDA for two minutes and then injected and separated by MEKC. (b) HeLa cell lysate labeled with NDA for one minute and then separated by MEKC. The inset was generated using an identical protocol, but with no lysate, and the Y-axis was scaled identically to that of the main panel. Peaks were assigned by spiking with NDA labeled standards.

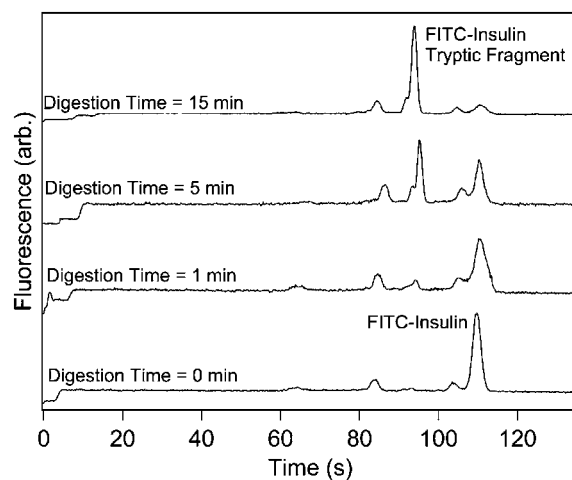


Fig. 5 Electropherograms generated by on-chip digestions of singly labeled FITC-Insulin (offset vertically for clarity). As shown, as the digestion progresses for longer periods, peak(s) representing tryptic digest fragment(s) appear at 94 s, and the parent FITC-Insulin peak at 110 s disappears. After fifteen minutes the digestion has neared completion.

detectable species. Droplets containing FITC-Ins were merged with droplets containing trypsin and incubated for different periods prior to being driven to the interface to be sampled into

the microchannels. Upon injection into the channels, the reaction was quenched, as the surfactant denatures the enzyme; thus, this serves as a metric for monitoring reaction progress as a function of time. Fig. 5 shows four electropherograms generated after progressively longer digestion times. As shown, as digestion time increases, the primary FITC-Ins peak (retention time ~110 s) disappears, while a new peak belonging to a digest fragment appears at retention time ~94 s.

Tryptic digestion of FITC-Ins can create two labeled fragments through cleavage at the B-Chain Lys or B-chain Arg residues forming peptides that are 1- or 8-residues shorter than the parent molecule. The digest fragment peak in the electropherograms appears to have a shoulder which may correspond to detection of both fragments. Overall, the time required for complete digestion (~15 min) is short relative to conventional solution-phase digestion protocols which require longer times (~12 hours) and elevated temperature (37 °C).⁷ These results show great promise for our plans to build devices with much larger electrode arrays for integration of multistep proteomic processing regimens.³⁹

Conclusion

We have proposed, fabricated, and tested a hybrid device that integrates digital microfluidics with microchannels on one substrate. The hybrid device uses digital microfluidics to perform chemical processing on samples prior to transporting them to microchannels for analytical separations. The method was demonstrated to be capable of on-chip labeling of amino acids and amines in cell lysate, as well as enzymatic digestion of peptide standards, followed by MEKC separation in microchannels. We believe this marriage of digital microfluidics and microchannels is an important step toward fully integrated lab-on-a-chip for in-line sample processing and separation.

Acknowledgements

We thank Irena Barbulovic-Nad for assistance with cell culture. We acknowledge the Natural Sciences and Engineering Research Council (NSERC) and the Canadian Cancer Society (CCS) for financial support. M.A. and M.W.L.W. on thank the Ontario Graduate Scholarship program and A.R.W. thanks the Canada Research Chair program.

References

- 1 S. C. Jacobson, R. Hergenroder, L. B. Koutny and J. M. Ramsey, *Anal. Chem.*, 1994, **66**, 1114–1118.
- 2 D. Wu, J. Qin and B. Lin, *J. Chromatogr. A*, 2008, **1184**, 542–559.
- 3 N. Gottschlich, C. T. Culbertson, T. E. McKnight, S. C. Jacobson and J. M. Ramsey, *J. Chromatogr. B*, 2000, **745**, 243–249.
- 4 M. Brivio, R. H. Fokkens, W. Verboom, D. N. Reinhoudt, N. R. Tas, M. Goedbloed and A. Van den Berg, *Anal. Chem.*, 2002, **74**, 3972–3976.
- 5 S. C. Jacobson, R. Hergenroder, A. W. Moore, Jr. and J. M. Ramsey, *Anal. Chem.*, 1994, **66**, 4127–4132.
- 6 K. W. Ro, K. Lim, H. Kim and J. H. Hahn, *Electrophoresis*, 2002, **23**, 1129–1137.
- 7 M. P. Washburn, D. Wolters and J. R. Yates III, *Nat. Biotechnol.*, 2001, **19**, 242–247.
- 8 H. J. Crabtree, E. C. S. Cheong, D. A. Tilroe and C. J. Backhouse, *Anal. Chem.*, 2001, **73**, 4079–4086.
- 9 D. Sinton and D. Li, *Colloids Surf., A*, 2003, **222**, 273–283.
- 10 G. M. Walker and D. J. Beebe, *Lab Chip*, 2002, **2**, 131–134.
- 11 M. A. Unger, H. P. Chou, T. Thorsen, A. Scherer and S. R. Quake, *Science*, 2000, **288**, 113–116.
- 12 G. T. Roman and R. T. Kennedy, *J. Chromatogr. A*, 2007, **1168**, 170–188.
- 13 S.-Y. Teh, R. Lin, L.-H. Hung and A. P. Lee, *Lab Chip*, 2008, **8**, 198–220.
- 14 J. S. Edgar, C. P. Pabbati, R. M. Lorenz, M. He, G. S. Fiorini and D. T. Chiu, *Anal. Chem.*, 2006, **78**, 6948–6954.
- 15 G. T. Roman, M. Wang, K. N. Shultz, C. Jennings and R. T. Kennedy, *Anal. Chem.*, 2008, **80**, 8231–8238.
- 16 M. G. Pollack, R. B. Fair and A. D. Shenderov, *Appl. Phys. Lett.*, 2000, **77**, 1725–1726.
- 17 J. Lee, H. Moon, J. Fowler, T. Schoellhammer and C.-J. Kim, *Sens. Actuators, A*, 2002, **95**, 259–268.
- 18 I. Barbulovic-Nad, H. Yang, P. S. Park and A. R. Wheeler, *Lab Chip*, 2008, **8**, 519–526.
- 19 V. N. Luk, G. C. Mo and A. R. Wheeler, *Langmuir*, 2008, **24**, 6382–6389.
- 20 E. M. Miller and A. R. Wheeler, *Anal. Chem.*, 2008, **80**, 1614–1619.
- 21 D. Chatterjee, B. Hetayothin, A. R. Wheeler, D. J. King and R. L. Garrell, *Lab Chip*, 2006, **6**, 199–206.
- 22 V. Srinivasan, V. K. Pamula and R. B. Fair, *Lab Chip*, 2004, **4**, 310–315.
- 23 D. Brassard, L. Malic, F. Normandin, M. Tabrizian and T. Veres, *Lab Chip*, 2008, **8**, 1342–1349.
- 24 S. K. Cho, H. Moon and C. J. Kim, *J. MEMS*, 2003, **12**, 70–80.
- 25 M. Abdelgawad and A. R. Wheeler, *Adv. Mater.*, DOI: 10.1002/adma.200802244.
- 26 A. R. Wheeler, *Science*, 2008, **322**, 539–540.
- 27 F. Malloggi, H. Gu, A. G. Banpurkar, S. A. Vanapalli and F. Mugele, *Eur. Phys. J. E*, 2008, **26**, 91–96.
- 28 W. Satoh, H. Hosono and H. Suzuki, *Anal. Chem.*, 2005, **77**, 6857–6863.
- 29 W. Satoh, H. Yokomaku, H. Hosono, N. Ohnishi and H. Suzuki, *J. Appl. Phys.*, 2008, **103**, 034903.
- 30 D. Huh, A. H. Tkaczyk, J. H. Bahng, Y. Chang, H. H. Wei, J. B. Grotberg, C. J. Kim, K. Kurabayashi and S. Takayama, *J. Am. Chem. Soc.*, 2003, **125**, 14678–14679.
- 31 U.-C. YiW. LiuP.-P. d. Guzman and C.-J. Kimin, *Proceedings of 2006 Hilton Head Solid-State Sensor, Actuator and Microsystems Workshop*, IEEE, Piscataway, NJ, 2006, pp. 128–131.
- 32 D. C. Duffy, J. C. McDonald, O. J. A. Schueller and G. M. Whitesides, *Anal. Chem.*, 1998, **70**, 4974–4984.
- 33 M. Abdelgawad and A. R. Wheeler, *Adv. Mater.*, 2007, **19**, 133–137.
- 34 C. Cooney, C.-Y. Chen, M. Emerling, A. Nadim and J. Sterling, *Microfluid. Nanofluid.*, 2006, **2**, 435–446.
- 35 J. Berthier, *Microdrops and digital microfluidics*, William Andrew Pub. Norwich, NY, 2008.
- 36 K. Sueyoshi, F. Kitagawa and K. Otsuka, *J. Sep. Sci.*, 2008, **31**, 2650–2666.
- 37 Z. Long, Z. Shen, D. Wu, J. Qin and B. Lin, *Lab Chip*, 2007, **7**, 1819–1824.
- 38 W. Yang, X. Sun, T. Pan and A. T. Woolley, *Electrophoresis*, 2008, **29**, 3429–3435.
- 39 M. Jebrail and A. R. Wheeler, *Anal. Chem.*, 2009, **81**, 330–335.